Evaluation of the Effect of the Loss of Adhesion of The Geosynthetic Interface-Asphaltic Mixture in the Performance of a Flexible Pavement Using the Technique of Numerical Modeling*

Lucio Cruz[**]
Mauro Realpe[***]
Jaime Obando[****]

Received: 20/07/2020 • Accepted: 08/07/2022
https://doi.org/10.22395/rium.v21n41a3

Abstract

Different numerical simulations were carried out based on finite elements, where the response of six different pavement structures subjected to the effects of the load of an equivalent axis is analyzed, where a geogrid was placed in the asphalt layer as reinforcement. For the reinforcement geogrid, there are different adherence characteristics between the geosynthetic and the asphalt mixtures, in such a way that the performance of the systems was evaluated when absolute roughness is present at the interface, and roughness coefficients of 0.9, 0.7 and 0.5. The results obtained were compared with the responses of the structures without reinforcement, in this way the performance that was presented was studied to determine how critical the progressive loss of adherence is when implementing the geogrid as reinforcement in the wearing course. As a conclusion, it is found that the loss of adherence geogrid-asphalt layer produces a fundamental loss of structural response capacity, with a performance even worse than the case without any reinforcement.

Keywords: geosynthetic; interface; adherence; roughness coefficient; flexible pavement; absolute roughness.

* Article is a product of the finished thesis to obtain the title of Master in Pavements Engineer. Text title: Evaluation of the effect of the loss of the adhesion of the geosynthetic interface - asphaltic mixture on the performance of flexible pavement using the technique of numerical modeling at the University of Cauca, 2018-2019.

** Ph.D. and Msc. in Engineering, Faculty member at Civil Engineer Faculty, Department of Geotechnics, University of Cauca, Colombia. E-mail: lucruz@unicauca.edu.co. Orcid: http://orcid.org/0000-0003-2438-5526

*** Engineer Msc. Pavement Student, Civil engineer faculty, University of Cauca, Colombia. E-mail: maurorealpe@unicauca.edu.co Orcid: https://orcid.org/0000-0003-1751-8562

**** Ph.D. and Msc. in Engineering, Faculty member at Civil Engineer Faculty, Department of Geotechnics, University of Cauca, Colombia. E-mail: jaimeobando@unicauca.edu.co. Orcid: https://orcid.org/0000-0003-0540-7021

Evaluación del efecto de la pérdida de la adherencia de la interfaz geosintética-mezcla asfáltica en el desempeño de un pavimento flexible utilizando la técnica de la modelación numérica

Resumen

El presente trabajo muestra diferentes simulaciones numéricas basadas en elementos finitos, donde se analiza la respuesta de seis diferentes estructuras de pavimento sometidas a los efectos de la carga de un eje equivalente donde en la carpeta asfáltica se colocó una geomalla como refuerzo. Para la geomalla de refuerzo se tienen diferentes características de adherencia entre la geosintética y las mezclas asfálticas, evaluándose el desempeño de los sistemas cuando se tiene en la interfaz rugosidad absoluta y coeficientes de rugosidad de 0.9, 0.7 y 0.5. Los resultados que se obtuvieron se compararon con las respuestas de las estructuras sin refuerzo, de esta manera se estudió el desempeño que presentaba la estructura del pavimento al incorporar la geomalla como elemento de refuerzo y diferentes niveles de adherencia. Como conclusión, se encontró que la perdida de adherencia geomalla-carpeta asfáltica produce una pérdida de capacidad estructural, que incluso supera una condición sin presencia de refuerzo.

Palabras clave: geosintético; interfaz; adherencia; coeficiente de rugosidad; pavimento flexible; rugosidad absoluta

INTRODUCTION

The use of geosynthetics has become slowly popular in last decades, being used to provide different solutions on the engineering field. Such elements are used generally as layers, dividers, filters, drains, reinforcements, protective layers, and protection barriers [1]. Its use is very common in pavement to reinforce the subsurface [2], in such way that if the ground does not fill minimum load conditions, geogrid helps to significantly relieve the coming stress. On the other hand, about pavement rehabilitation, these elements are placed as a coating between old and new asphaltic layers working as reinforcement [3] to achieve more durability [4], [5]. When pavements are built, geosynthetics can be use in such way that the asphalt layer is divided in two parts and the element placed in between as reinforcement.

On new or rehabilitation pavement projects, geosynthetics are also used to delay fissures over the new asphalt layers which are coming from existent underneath layers. Its use implies an interphase between new and old pavement layers and the geogrid [6-7]. The ideal is that when these solutions are offered, the union between materials should be a monolithic one in order to confront external stress to which they will be subjected to on the new pavement structure. This is achieved by guaranteeing an appropriate adherence between layer of the new structure pack, therefore allowing for the pavement to have a longer lifespan [8]. If this is not guaranteed, the pavement could fail because of its adherence [9] [10] [11].

According to geosynthetics manufacturers, these elements allow improvements in the different layers' performance, however, there isn't a designed method with scientific support to elaborate such systems because they are made empirically, therefore, the reason why asphaltic layers and geosynthetic begin losing adherence through time [12].

Considering this panorama, it is interesting to deepen in the study of adherence phenomena when using geogrid as a reinforcement when building or rehabilitating pavement. An ideal tool to further analyze this problem is using numeric modeling [13], which allows to study such structures' behavior, therefore, to analyze the fatigue performance the pavement suffers when loss of adherence occurs due to vehicle load [14].

1. MATERIALS AND METHODS

1.1 Selection of Pavement Structure

Chapter 8th of the Asphaltic Pavement Design Manual, —about medium to high transit volume in Colombia [15]— shows 6 types of design charts organized according to

different conditions throughout the regions in the country. This manual brings into account variables like weather conditions (R), transiting levels (T), ground resistance conditions to build a sub-surface (S), and defined material characteristics for each layer. This, with the goal to offer diverse pavement structures according to the selected region to build upon, guaranteeing the availability of materials in the region, and the respective economic analysis of alternatives.

Those structures provided by the manual were determined under AASHTO (American Association of State Highway and Transportation Officials) (1993) technology. From a total of 270, organized in 45 subgroups, only 6 of them were selected representing the total of groups and including a composition of: a dense hot mixture, a granular base and sub-base with the purpose of facilitate the coded characteristics into a software model based on finite elements.

Afterwards, it was noticed that selected models had different thickness layers, making it impossible to compare the inter-phase layers on pavement structures because they will be on different heights; then, and based on ASSHTO from 1993, thickness was modified in such way that its elasticity module was variable; therefore, all pavement structures parts had the same layer thickness to help in an accurate comparison.

Results can be observed in Figure 1 with the models worked on as simulators.

Figure 1. Selected pavement structures for simulations with its characteristic and properties displayed accordingly

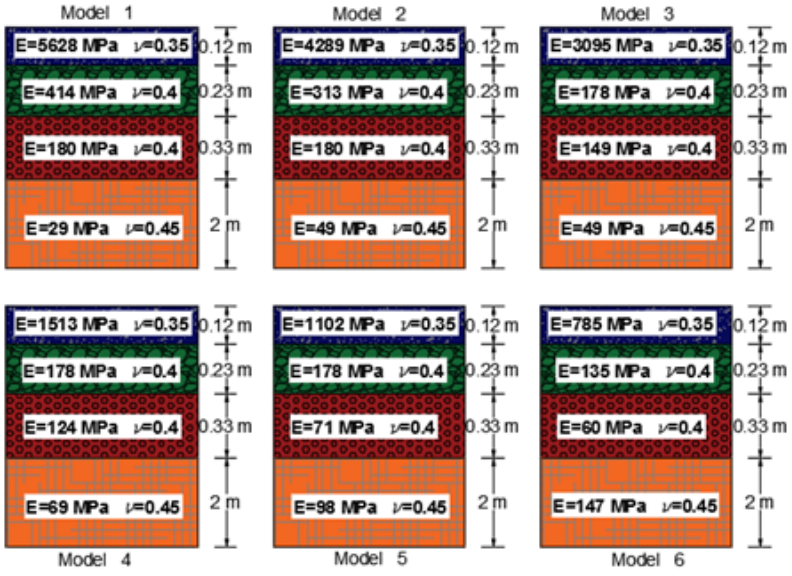

Source: own elaboration.

1.2 Reinforcement Material Selection (Geogrid)

To reinforce the previous 6 selected pavement structures, it was selected the use of a glass-fiber geogrid which, according to the manufacturer, is flexible and provides resistance on both directions.

Generally, they are used to control cracks due to flexion, fatigue, and plastic deformities on asphaltic pavement layers. These provide a bituminous covering, adding a fixed adhesion to asphaltic layers (over/ underneath) in such way to reduce to the highest the relative displacement between geogrid and asphaltic layers. To clarify, models were done corresponding to an elastic-linear constitutive model, therefore, the only properties to consider for the reinforcement element were: elasticity module (70,000 MPa, according to manufacture); Poisson coefficient, taken from previous research [14], with a value of v=0.35. Table 1 shows the technical specification for geogrid given by the manufacturer.

Table 1. Technical specifications of geogrid simulations

Properties	Units	R - 50	R - 100
Last tension resistance (ST/SL)	KN/m	50/50	100/100
Grinds' opening size (ST/SL)	mm	20/20	18/18
Width	m	3.95	3.95
Length	m	100	50

Source: own elaboration.

1.3 Modeling Methods

All the modeling was executed in a tri-dimension way in all selected structures. A 3.5 m lane was taken (axis X); height of 2.68 m (axis Z) and length of 10m (axis Y). Also, to analyze the system response, a constitutive elastic-lineal model was built and the properties of the material to study were the dynamic model for asphaltic layers, the resilient model for other layers; the Poisson coefficients and each material's density, all, with the purpose to consider their own weight on each pavement structure.

Each pavement structure was submitted to a load produced by a pair of tires with an equivalent axis [16], consisting of a double tire with 8.2 tons load. Each tire exerts a force of 2,050 kg over the asphaltic layer with a = 10.8 cm of circumference effect. Each pair of tires was separated to a distance of S = 3 a = 32.4 cm and produced a contact pressure of 5.6 $\frac{Kg}{cm^2} = 560000\ Pa$. Figure 2 represents the equivalent axis (left) and interest load for different models (right).

Figure 2. Equivalent axis characteristics (left) and, model loads (right)

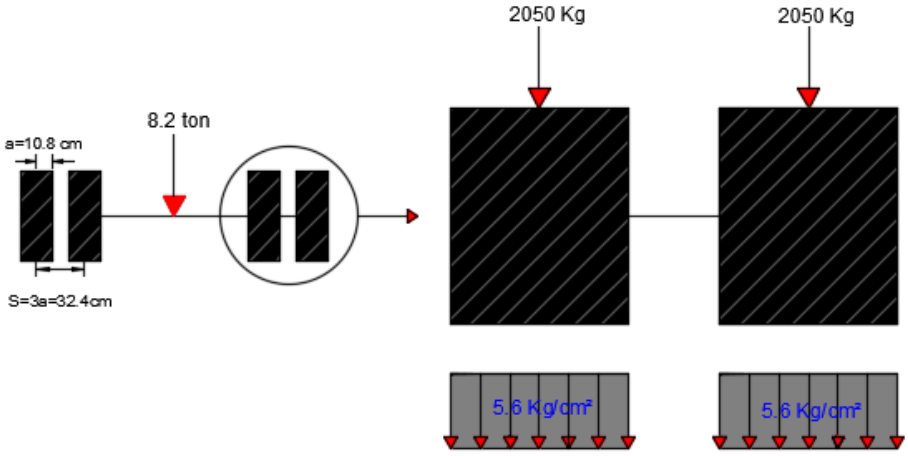

Source: own elaboration.

According to this, the effort made from each tire is 5.6 *Kg*/cm^2. Figure 3 exhibits how each structure is loaded on simulated pavement. Besides the previously described measurements, each model was subjected to half of the equivalent axis and such loads were placed centered over the model.

Figure 3. structural loads over 3D pavement model

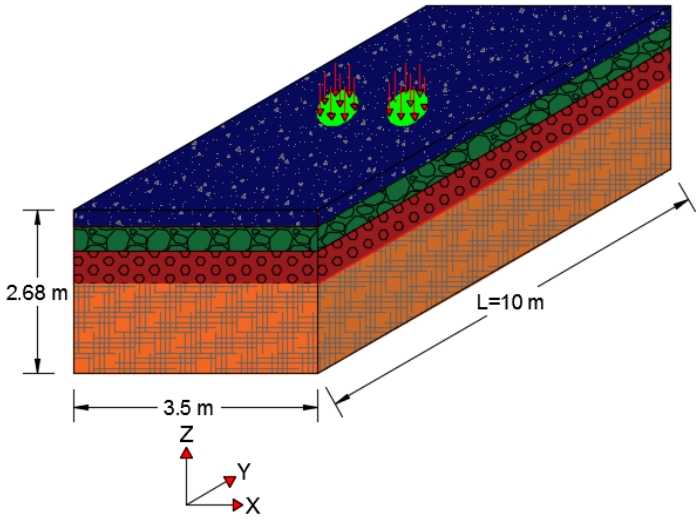

Source: own elaboration.

Six models were made without reinforcement with the intention to have reference values and to be compared to the results obtained after reinforcing the structures.

On each simulation, interacting layers had absolute roughness to avoid relative displacements along them. On each model, interest values were taken along the X axis (width of the system). Table 2 shows the variables considered and the places where measurements were taken.

Table 2. Model measurements taken on no-effort variable

Place	Variable
Underneath layer	Unit deformation on X
	Unit deformation on Y
	Stress on X
	Stress on Y
	Desplacement on X
	Displacement on Y
Superior sub-surface	Stress on X
	stress Z
	Displacement on Z

Source: own elaboration.

Afterwards, the setting of other models was carried out with a stress element, assuming a pavement rehabilitation located between a new asphaltic layer (layer 1) and an old one (layer 3). It must be remembered that the thickness of the layer on the non-stress model is 12 cm; that is the reason why it was decided to locate the geogrid over 8 cm depth, corresponding to less than ¾ of such thickness. Layer 1 was thicker causing more pressure on its underneath layer and for the geogrid, assuming the greatest stress —as it acts in a similar way as a simple leaned beam where steel acts as the reinforcement—, it is placed close to the bottom part, because is the position where the greatest stress-tension is assumed.

Figure 4. Structure of pavement reinforcement model

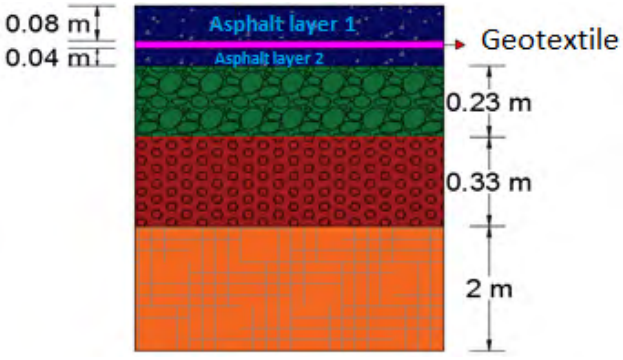

Source: own elaboration.

It must be clarified that all interactions along surfaces with different contact-granulated materials were considered like they were absolutely rough, that is to avoid relative displacement along them. However, regarding the geogrid surface interaction on —over and under rows—, layers 1 and 2 were different with the goal of analyzing the structures' performance when friction on the interface is losing its adherence progressively. Therefore, 6 models were made considering the surface of the geosynthetic on its setting of absolute roughness; 6 additional with a friction coefficient of $\mu = 0.9$; another 6 with $\mu = 0.7$ friction; and, finally, another group of 6 with more $\mu = 0.5$ [3], for a total of 24 simulations under and without stress.

Location points where values were taken were the same centered ones used at the no-stress analysis, however, for this situation, they will be quantified underneath the rs 1 and 2. Table 3 shows variables for each analysis and measured spot.

Table 3. Measured places for under-stress models

Location	Variable
Underneath layer 1	Unit deformation on X
	Unit deformation on Y
	Stress on X
	Stress on Y
Underneath layer 2	Unit deformation on X
	Unit deformation on Y
	Stress on X
	Stress on Y
	Displacement on X
	Displacement Y
Upper sub-surface	Stress on X
	Stress on Z
	Displacement on Z

Source: own elaboration.

One of the fundamental variables when designing flexible pavement is the unit deformation along traffic flow [16]. For the coordinate system taken on this exercise and on the software, would be the unitary deformation on Y, which is the fatigue on pavement due to its greater tension effort which will present the same direction over the asphaltic layer. This deformity will be the main one to look for to avoid the pavement showing stress failure [17] [18], or at least that value on this variable on 6 models was expected when reducing the use of the geogrid structure.

Because of that, the approach was to calculate the equivalent transit corresponding to each model from the unitary deformations on Y, measured on software through infinite elements. The theoretical model used to calculate will be the one offered by the laws of fatigue from the Asphalt Institute [18], described forward.

$$N = 0.00432 K_1 C * (\frac{1}{\varepsilon})^2 * (\frac{1}{E})^3 \quad (1)$$

Where:

N_f= Equivalent transit

E = Módule of elasticity on layer [PSI]

ε_t = Unit deformation along trafic on critical spot

K_1 = 18.4

K_2 = 3.291

K_3 = 0.854

$$C = 10^M \quad (2)$$

$$M = 4.84 * (\frac{V_b}{V_a + V_b} - 0.6875) \quad (3)$$

V_b = Asphalt mixture volume percentage

V_a = Air mixture volume percentage

According to selected models on pavement manual, to elaborate mixtures with asphaltic concrete, hot-dense mixtures were made (HDM) to which a value of asphaltic volume of and air on mixture of:

$$V_a = 5\ \% \quad ; \quad V_b = 12.5\ \%$$

Applying the previous law, it would be possible to analyze the performance on different pavement structures once the reinforcement was placed and harshness coefficients were handled.

2. RESULTS

2.1 Results for Underneath Layer 1

It is important to highlight that the term "layer 1" is only present on models with geogrid treatment as it is considered for pavement rehabilitation. Layer 1 refers to the new coat

and “layer 2” for the former one. Like this, then, the segment show the response to 2 determined models as: 1 and 6; given that 2, 3, 4, and 5 showed similar results. The variables displayed belong to the unitary deformation on X and Y taken from underneath layer 1. Figures 5 and 6 have the captured results for model 1 $E_{Layer} = 5628\,MPa$).

Figure 5. Lane width vs X unitary deformation on layer 1. E=5628 MPa model

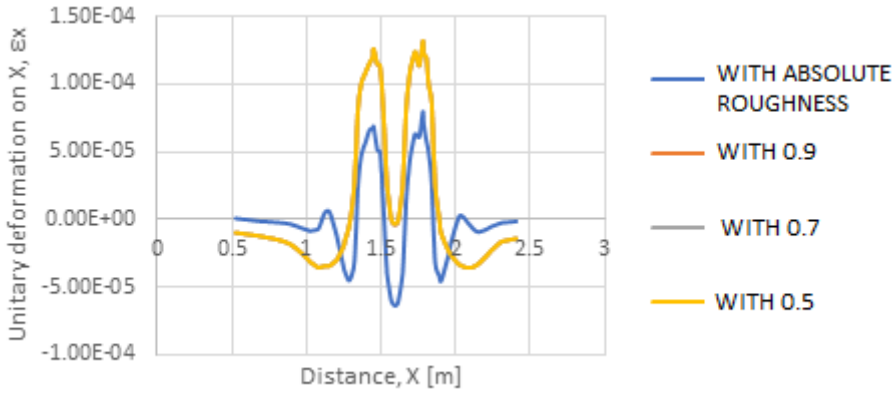

Source: own elaboration.

Figure 6. Lane width vs. unitary deformation on Y. Layer 1 for model E=5628 MPa

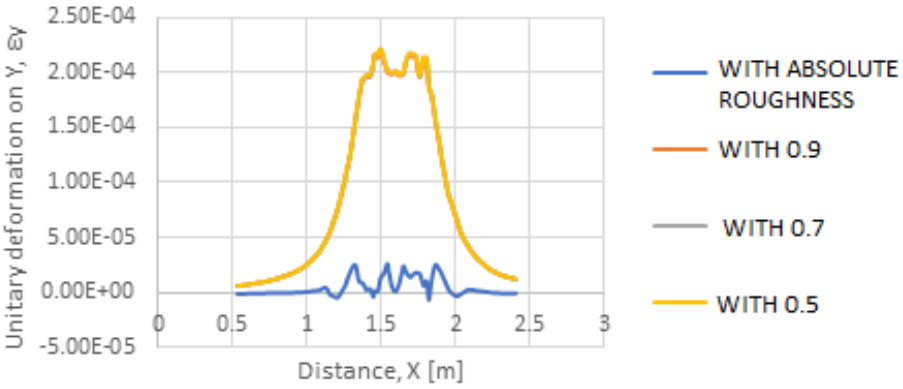

Source: own elaboration.

Likewise figures 7 and 8 show the same results, but for model 6, ($E_{Layer} = 785\,MPa$):

Figure 7. Lane width vs unitary deformation on X. Layer 1 for model 6, E=785 MPa

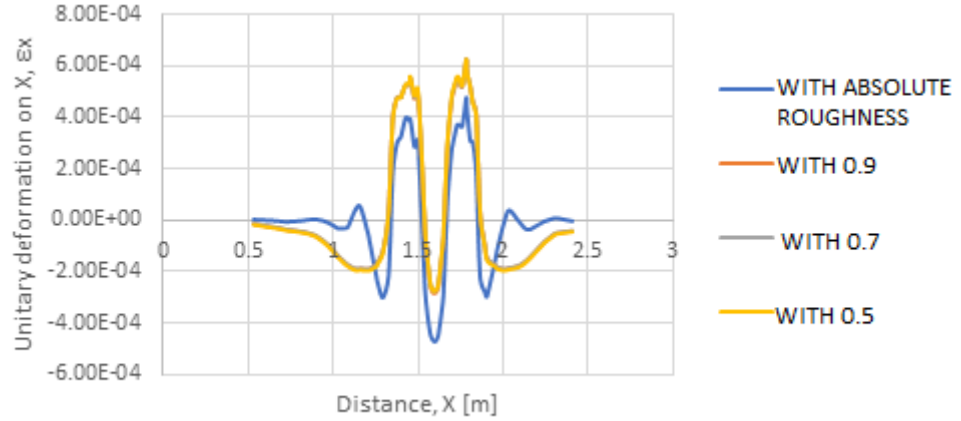

Source: own elaboration.

Figure 8. Lane width vs unitary deformation on Y. Layer 1 to model 6 with E=785 MPa

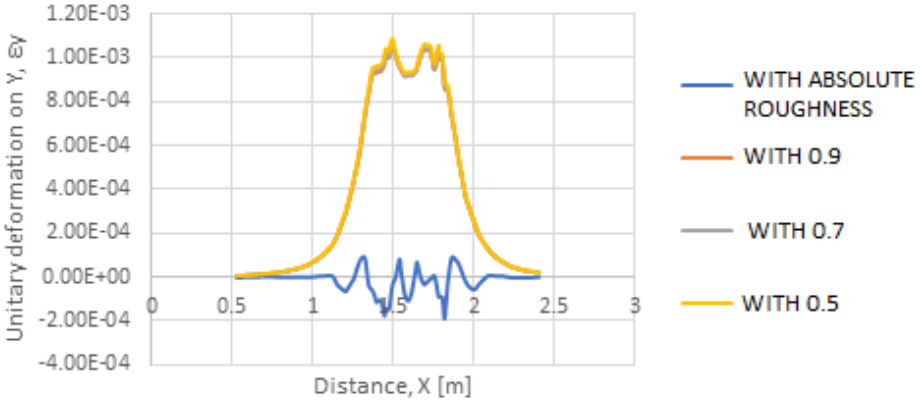

Source: own elaboration.

2.2 Results Underneath Layer 2

The following figures show the response to variables unitary deformation and displacement on X and Y on a given section over the lanes. Here are included the obtained results from non-reinforced to establish a comparison about the depth they are measured of all variables; therefore, figures 9 to 12 show results for model 1 ($E_{layer} = 5,628\,MPa$).

Figure 9. Lane width vs. unitary deformation on X. Layer 2 for E=5628 MPa model

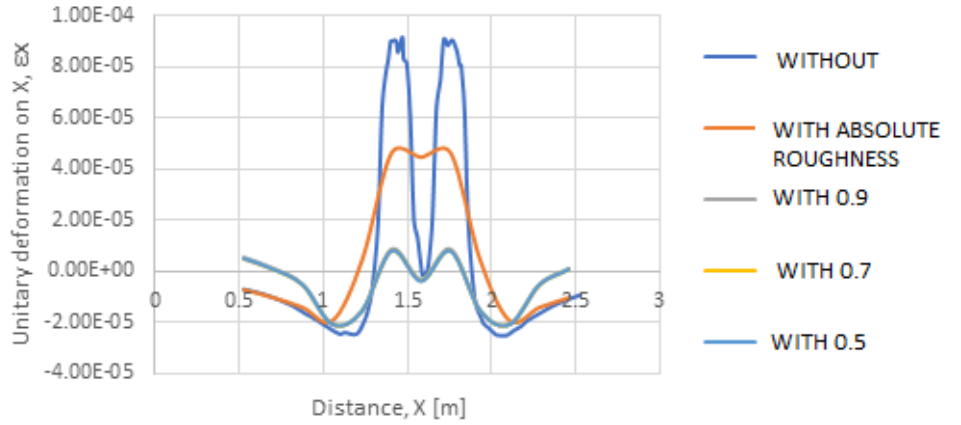

Source: own elaboration.

Figure 10. Lane width vs unitary deformation on Y. Layer 2 for model E= 5628

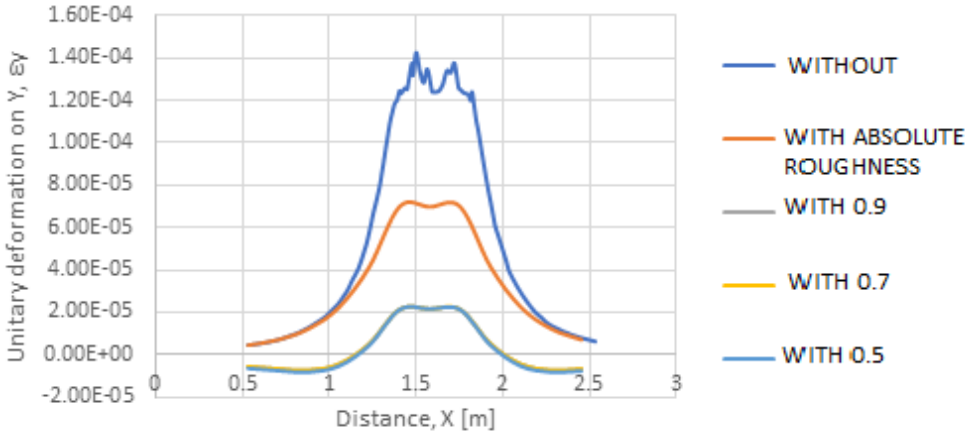

Source: own elaboration.

Figure 11. Lane width vs. displacement over X con layer 2. Model 1 E=5628 MPa

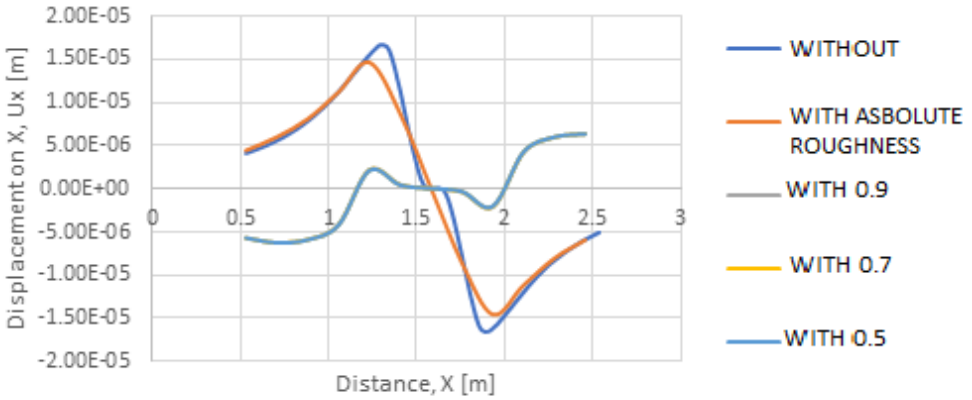

Source: own elaboration.

Figure 12. Lane width vs displacement on Y. Layer 2 for model 1, E=5628 MPa

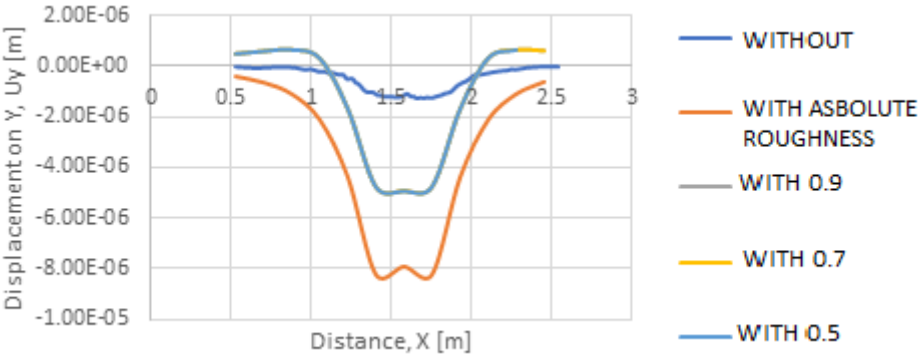

Source: own elaboration.

Same way, figures 13 to 16 show the graphics of the same variables for model 6 ($E_{layer} = 785\,MPa$).

Figure 13. Lane width vs unit deformation on X. Layer 2, Model 6 with E=785 MPa

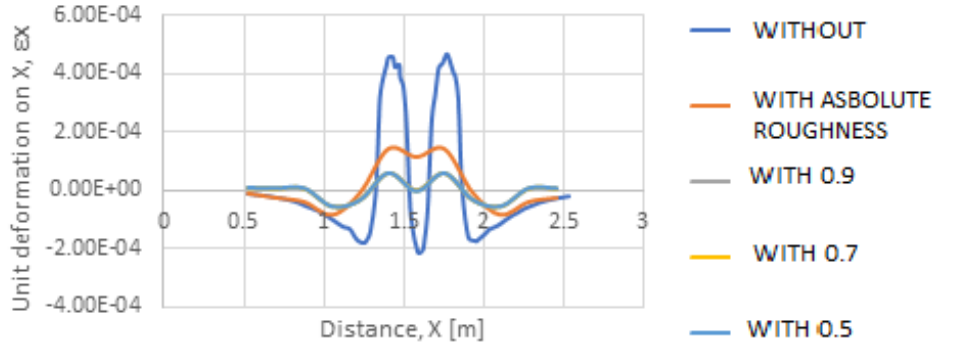

Source: own elaboration.

Figure 14. Width of lane vs displacement on Y. Layer 2 for model 6 with E=785 MPa

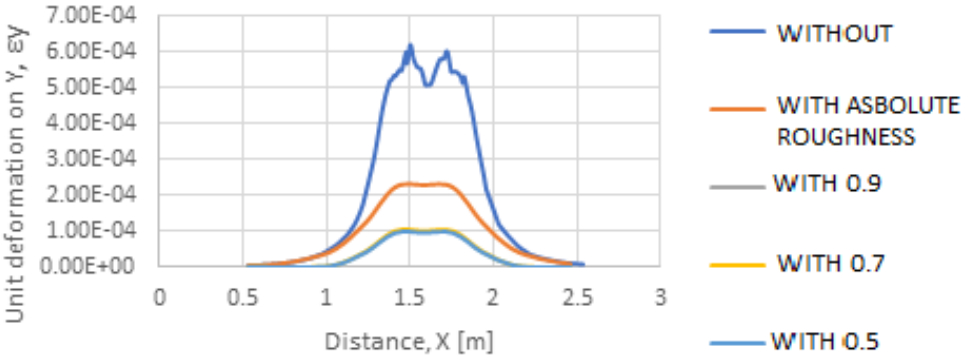

Source: own elaboration.

Figure 15. Lane width vs displacement on Y. Layer 2, model 6 with E=785 MPa

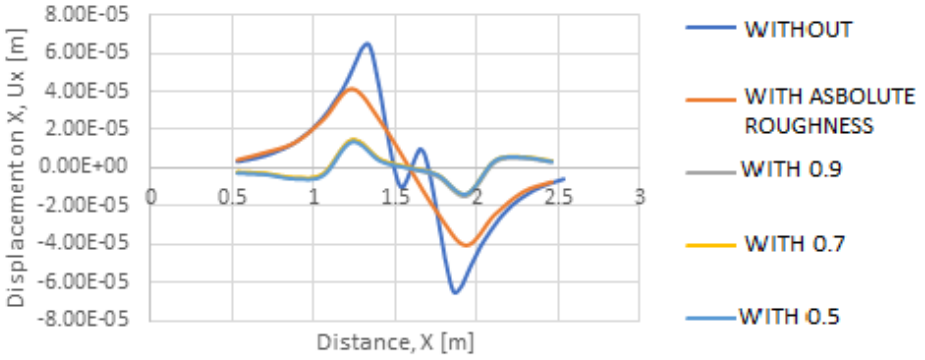

Source: own elaboration.

Figure 16. Lane width vs displacement on Y. Layer 2, model 6 with E=785 MPa

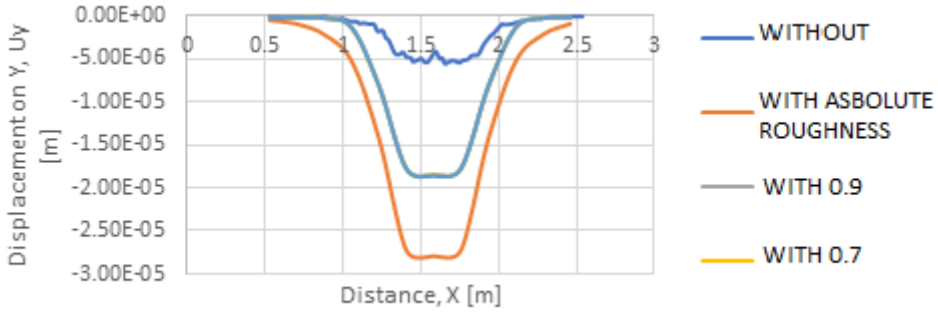

Source: own elaboration.

2.3 Results on Upper Sub-Surface

It was decided to take some values of the upper side of the sub-surface with the purpose of looking if the adherence loss on upper layers [19] produces an altering effect of performance over rutting, that is why measurements were taken on vertical displacements over the lane's width. Figure 17 exhibits the graphics for model 1 ($E_{layer} = 5,628\,MPa$).

Figure 17. Lane width vs vertical displacement on sub-surface. Model 1 with E=5628 MPa

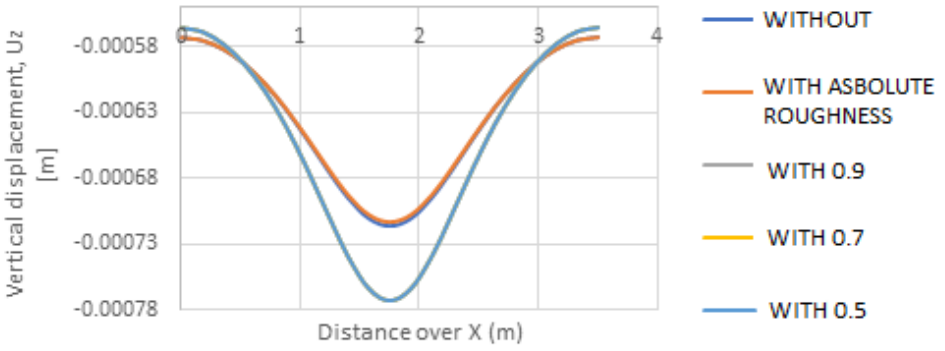

Source: own elaboration.

The next figure (18) shows the same previous graph but for model 6 ($E_{layer} = 785\,MPa$).

Figure 18. Lane width vs. vertical sub-surface displacement, Model 1, E=785 MPa

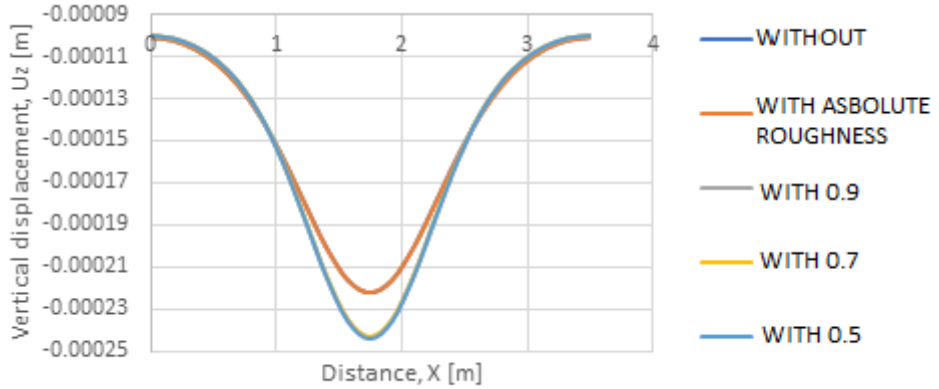

Source: own elaboration.

2.3.1 Comparative Results on with/without Reinforcement Over Depth Function

The present segment shows the values of unit deformation on X and Y from the same models as the base, in such a way that it allows taking a look at the existing change on structures with and without reinforcement under different roughness conditions. Results about such depth function for model 1 (E=5628 MPa) are shown in figures 19 to 22.

Figure 19. Unit deformation on X vs Depth for model 1 ($E_{layer} = 5628\,MPa$)

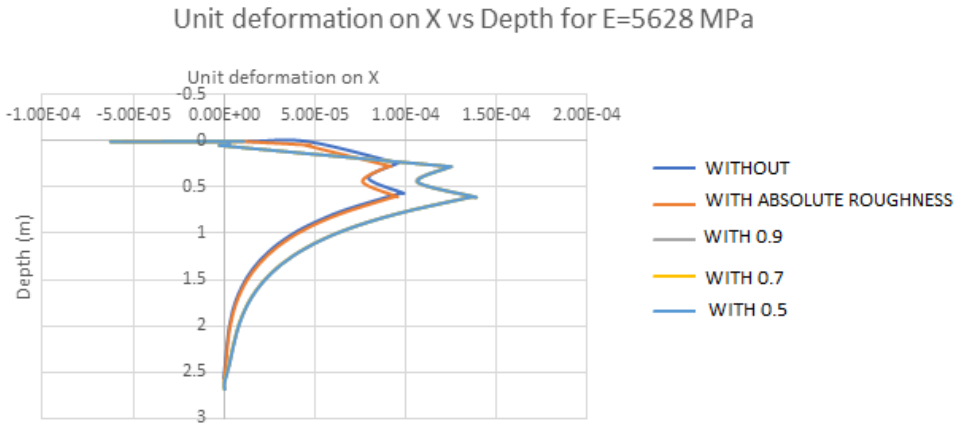

Source: own elaboration.

Figure 20. Unit deformation on Y vs depth. Model 1 ($E_{layer} = 5628\,MPa$)

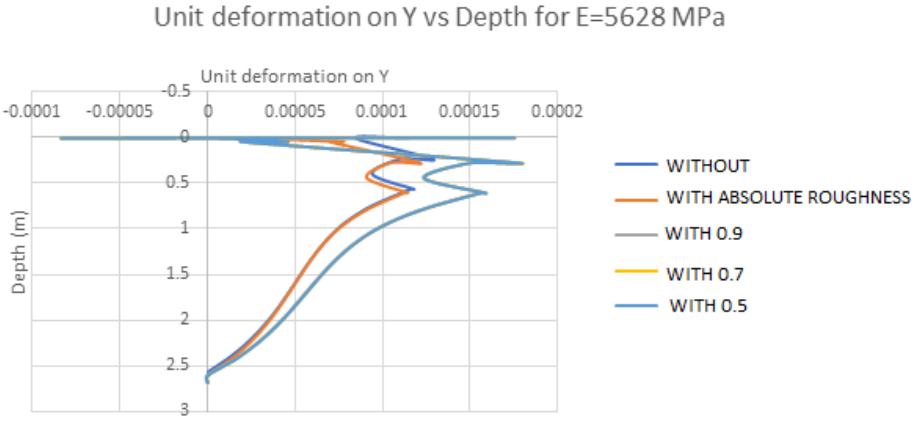

Source: own elaboration.

Figure 21. Unit deformation on X vs Depth. Model 1 ($E_{layer} = 785\ MPa$)

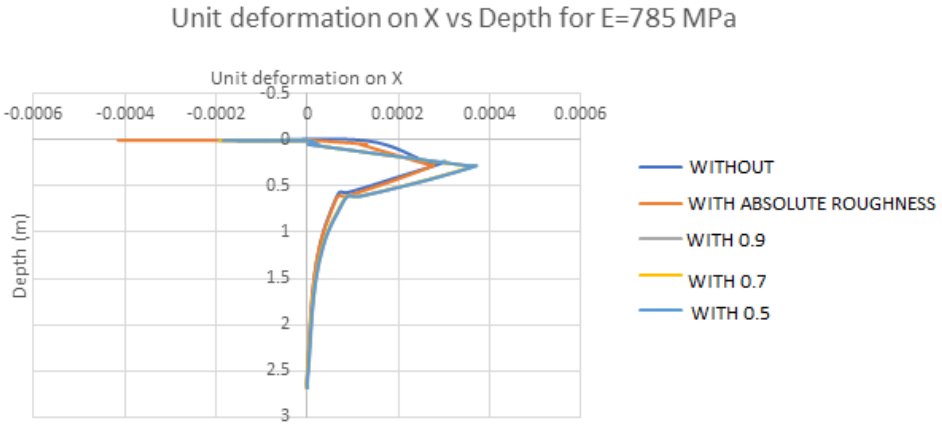

Source: own elaboration.

Figure 22. Unit deformation on Y vs Depth. Model 1 ($E_{layer} = 785\ MPa$)

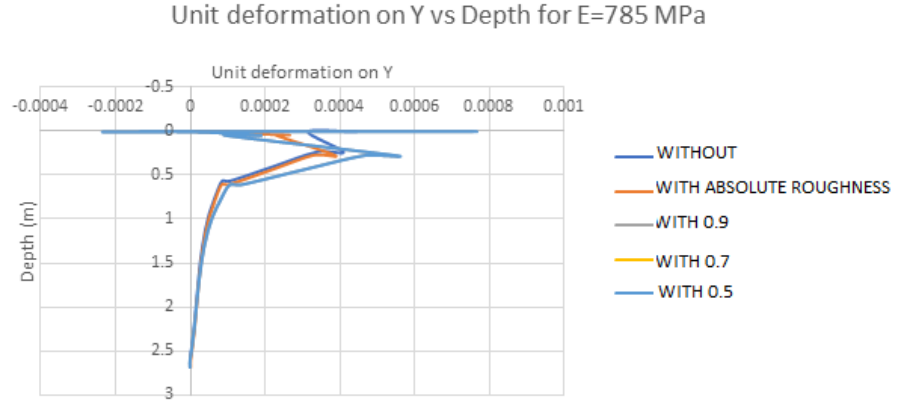

Source: own elaboration.

2.4 Admissible Transit Results

It must be remembered that the most important variable to consider about deformation is the direction of traffic because, according to fatigue's law from the Asphalt Institute, is the one generating fractures from bottom to top, producing the failure known as crocodile skin. Therefore, the maximum value for each model is determined by how much it increased or decreased such value according to models without reinforcement. The measurements and calculations on the improvement or failure percentages underneath layer 1 are shown in table 4.

Table 4. Improvement percentage of unit deformation on Y, underneath layer 1 against no reinforcements model

Model	Structure number (SN)	Abosolute roughness	0.9	0.7	0.5
		Improvement %	Failure %	Failure %	Failure %
1	6.65	81.6	35.4	35.5	35.7
2	5.76	82.3	34.2	34.4	34.5
3	5.07	84.8	30.7	31.0	31.3
4	4.21	85.3	37.3	37.8	38.2
5	3.23	84.9	42.2	42.8	43.3
6	2.3	85.4	41.5	42.3	43.0

Source: own elaboration.

Table 5 shows the improvement or worsening of the unit deformation over traffic direction on each model, regarding the values taken on the non-reinforcement model.

Table 5. Improvement or worsening percentage of unit deformation on Y according to underneath layer 2 on non-reinforcement models

Model	Structural Number (SN)	Absolute roughness	0.9	0.7	0.5
		Improvement %	Failure %	Failure %	Failure %
1	6.65	51.1	85.0	85.0	85.0
2	5.76	53.1	81.0	81.0	81.0
3	5.07	53.7	75.4	75.4	75.3
4	4.21	60.0	81.9	81.9	81.9
5	3.23	61.4	86.0	86.1	86.2
6	2.3	63.0	84.0	84.1	84.1

Source: own elaboration.

After the greatest values were selected among layers 1 and 2 for each model, with the goal of obtaining more critical conditions, the admissible transit for each model values were calculated. The results obtained can be seen on figure 23.

Figure 23. Elasticity module on layer vs. Admissible transiting

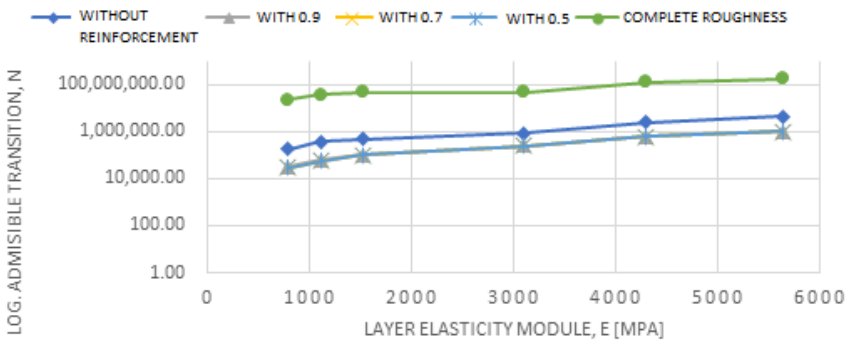

Source: own elaboration.

3. DISCUSSION

3.1 About Asphaltic Layers

On every image exhibited previously, it is possible to notice that curves had roughness coefficients looking like overlapping but, when zooming in, there is a slight difference between each curve, always with the same simulations of roughness coefficients of $\mu = 0.5$ with more unfavorable results as expected.

That apparent overlapping happens because when the interface of the geogrid-layer fails where the reinforcement is located, it shows a failure plane that produces discontinuity on stress the blocks generated when loads are applied. This is well represented on figure 24, showing an approximation of such distribution of stress in full adherence (a) and loss of adherence (b).

Figure 24. Stress Blocks. Full adherence (a.) and loss of adherence (b.)

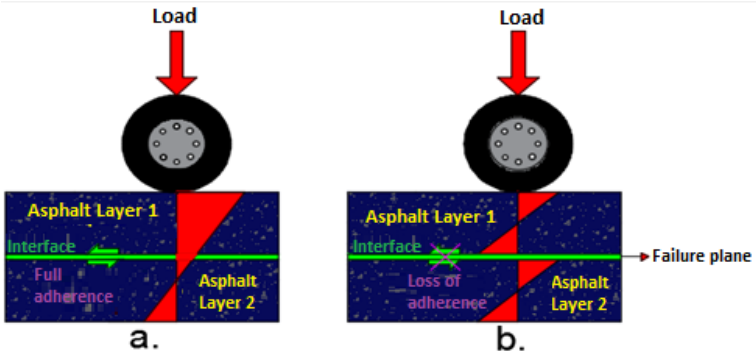

Source: own elaboration.

From the previous figure, one can infer that even though with roughness coefficients of different interface results are similar because of the loss of adherence –big or small– it means a new layer (layer 1) and an old one (layer 2) are not working monolithically [20][21], as an analogy to have two beams working separately. It is known that the greater the cant of a beam, the greater the resistance to required loads in such a way that if you have a system made by many beams or thick layers –appropriately laid one over the other, it would be less resistant as a monolithic beam of same the height. This can be demonstrated through the flexion theory [20][21] where the beam tension is directly proportional to the flexing moment (M) and inversely proportional to the resistance module (W) as such module may also be directly proportional to its height square as shown below:

$$\sigma_{\max} = \frac{M}{W} = \frac{M}{\frac{bh^2}{6}} = \frac{6M}{bh^2} \tag{4}$$

Because of this, it is determined that the higher (cant) the transversal section of the beam, the less the tension stress will be, better yet, the section will be more resistant. Then, it is established that is quite risky to use geogrid systems because, even at the time of building full adherence, there are many other factors that will age out the pavement and, through time, such adherence will be modified, generating the fact that the failure plane might have an even worse effect without the geogrid.

Another variable to consider is the inertia on the asphaltic layer, similar to a rectangular section where the value is directly proportional to the cant square of the section as shown in equation 5:

$$I = \frac{bh^3}{12} \tag{5}$$

Thus, if it is possible to guarantee the adherence between stress and asphaltic layers, it might be possible to optimize the section's durability.

According to figure 23, showing the admissible transit values to design conditions, it must always take the most critical values over the interest variables according to the location. In this case, the greater values of unitary deformation on Y, with absolute roughness, take place underneath layer 2 and when using any roughness coefficient (0.9, 0.7, 0.5) under layer 1. Therefore, to study their performance on such structures over traffic direction, the admissible axis amount that the structure could hold before failure must be calculated. Therefore, the improvement that it will present on pavement's durability is evident.

It is visible that with an adequate adherence (full roughness) between geogrid's glass fiber and asphaltic layers (new and old), its performance on each system is better

and the useful life is significantly better because it holds onto a greater repetition axis (equivalent axis) and its resistance against the failure by stress increases.

When studying the results obtained using a roughness coefficient, it is noticeable that it loses adherence, even a little (μ=0.9) resistance of the structure decreases instead of improving in relation to the non-stress models. This happens because the interface grid layer presents a failure plane generating a considerable lowering of inertia and producing early fissures.

Figure 25 displays a comparison of the diagram of an outlined model with no reinforcement (left) and one with full adherence reinforcement (right), where it can be noticed how stress is distributed over pavement layers when there is no geogrid.

Figure 25. Comparation of outlined stress tensor [Pa] for models with and without full adherence

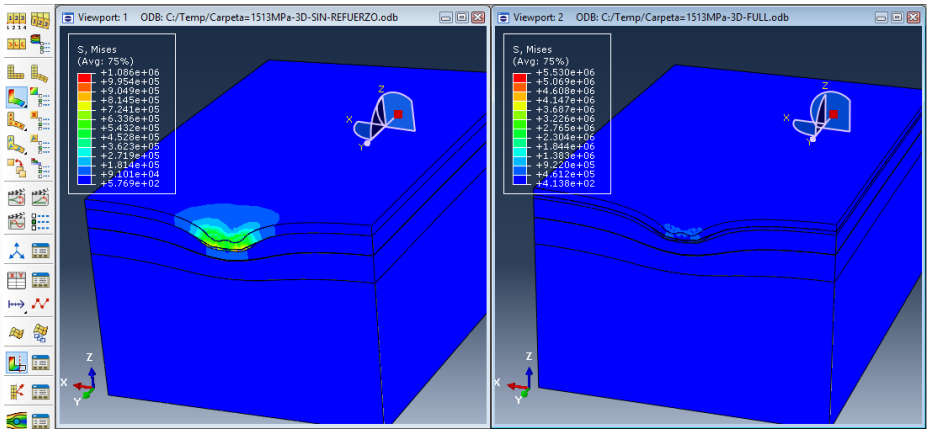

Source: own elaboration.

On the reinforced model it might look that such effects are significantly relieved of stress. To observe it better, a zoom-in on the geogrid was done, as seen in figure 26.

Figure 26. Load effect over geogrid for a full roughness model

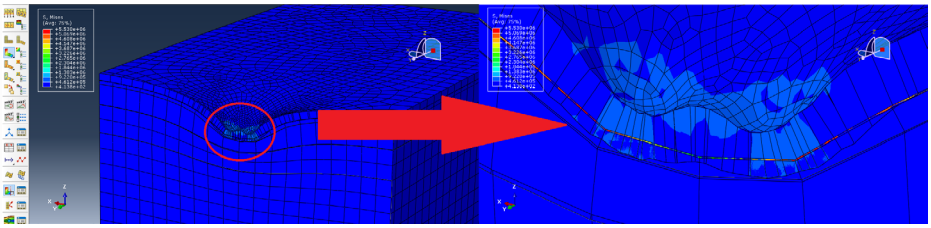

Source: own elaboration.

The figure above shows how greater efforts on geogrid are present because it is taking the greatest effect on the applied load as expected on the model. This happens

due to its high elasticity model because: if it had a greater system stiffness, it would also launch greater elastic energy.

Figure 27 shows the effect of installing the geosynthetic according to a displacement tensor. It can be observed on its values table that it has a reduction on the max value of this variable. Because the underneath value on the new layer is where it holds greater beneficial effects due to the reinforcement setting. Also, it is noticeable that with the geogrid, the energy over the bestowed load spreads better over the surrounding layers.

Figure 27. Comparison on diagramed tensor outlined from a displacement [m] for the model without (left) and with fully adhered reinforcement (right)

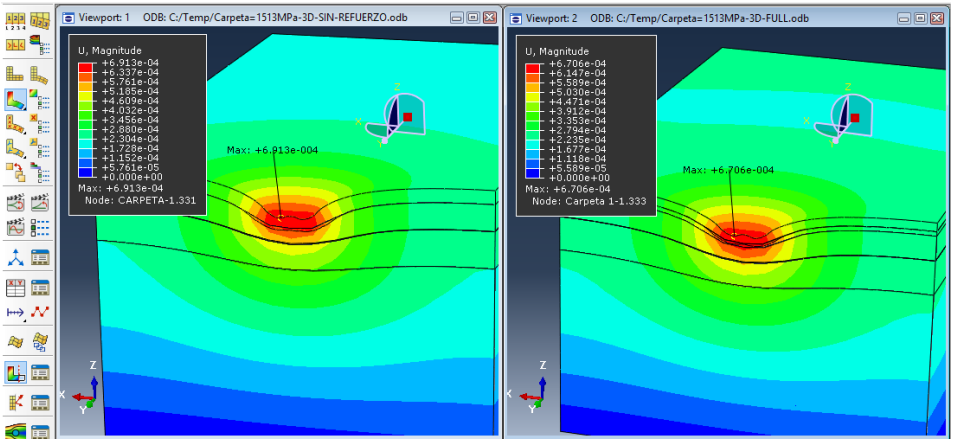

Source: own elaboration.

The unitary deformation on Y is the most important variable to include and figure 28 shows the comparison between both conditions: without (left), fully attached (middle) and one with a roughness coefficient of μ=0.5 (right).

Figure 28. Comparison between outlined tensor unitary deformation on Y. Left: without reinforcement. Center: Full cohesion reinforcement. Right: roughness coefficient reinforcement

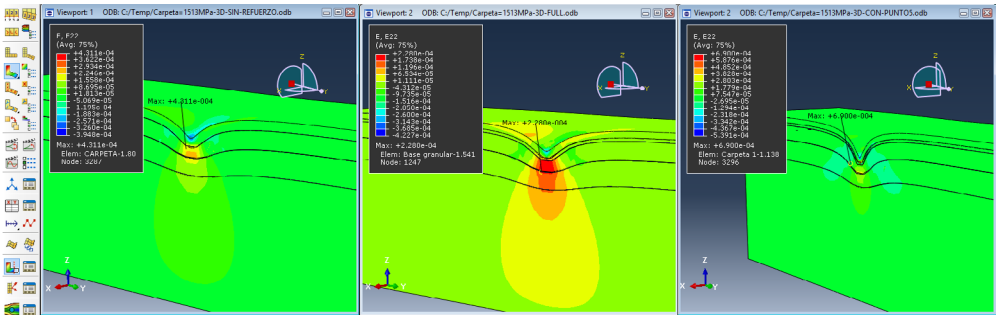

Source: own elaboration.

The figures above show how, when setting the geogrid, unit deformations on Y suffer an even re-distribution of stress due to both variables being proportional to Hooke's law: when spreading on a greater area, a reduction of max values is generated mostly into the half when compared to the with or without a model; different to when there is no stress or there is a full attach of roughness coefficient. These unit deformation values have the tendency to concentrate into a specific area which may cause a greater probability to present failures due to asphaltic layer stress. Moreover, it is observed on all three models that are in compression, negative values of the table (light blue), while the underneath of layer 2, the base and sub-base are at tension, just as the yellow extruding bulb shows in the diagram.

It must also be considered that greater values on layer 1 (under) will generate a possible early stress fissure. However, when adherence is efficient, it is visible that the energy spreads optimally on all the models, and that the highest values are lower than the asphaltic layer; more exactly, where there is no risk for the pavement to have stress failures, which means a greater appropriate service of pavement.

3.2 About Sub-Base

As would be expected, if the geogrid is set between asphaltic layers, its main effect will be reflected over the superior layers. When trying to improve the subsurface characteristics, what should be done is to place the reinforcement over this one. However, it can be noticed that it shows a slight improvement in the subsurface according to other variables (horizontal stress, vertical stress, and vertical displacement). Furthermore, it is important to consider vertical displacements because they are the ones that could bring failure because of rutting. In such a way, many values have a tendency to diminish, more specifically over absolute roughness, even though no geosynthetics are used to mitigate such fails, it is equally contributing to helping reduce big vehicle load over the subsurface.

On the other hand, it is evident that with weak adherence of the geogrid and asphaltic layers, displacements and vertical stress have the tendency to increase. That is: if no grid is placed correctly or if it loses adherence on the top layer through time, the resistance of the subsurface against rutting decreases and becomes even more prone to cracks.

3.3 About Subsurface

When implementing the fiberglass geogrid between the new and old layer with an appropriate adherence, the main effect is to be reflected in unitary deformation reduction on traffic direction (Y axis), the ones that are the cause of stress failures,

being this the main interest variable in this research. However, it is also noticeable that a slight improvement always happens over the upper subsurface regarding other variables (horizontal stress and vertical stress). The main one to consider is the vertical displacement which can fail due to rutting, meaning that the load capacity of the subsurface is not enough to hold on to vehicular transit, therefore, values can lower, specifically when it has absolute roughness. Figure 29 shows the result (green) of such effect, slightly noticeable because even though geosynthetics are not placed to mitigate these failures due to the natural composition of the grounds, it also helps to reduce the effects produced by vehicle loads over the subsurface.

Figure 29. Slight improvement on subsurface against rutting

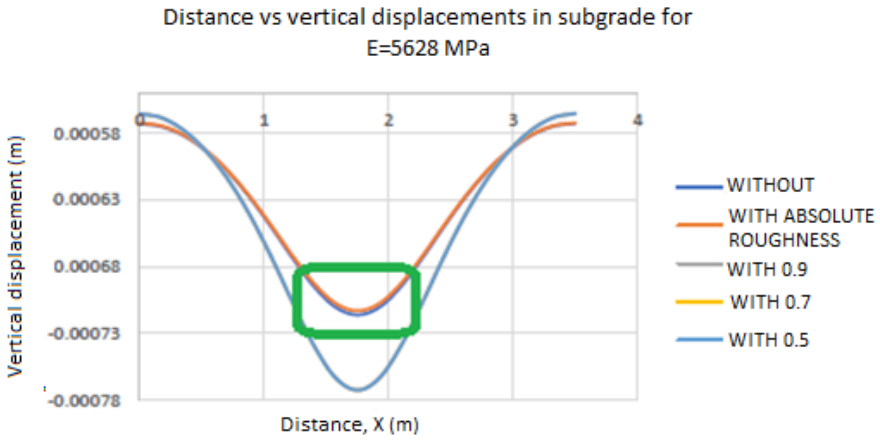

Source: own elaboration.

If an improvement were to be desired on the pavement foundation, a geogrid should be placed just underneath the subsurface for it to increase its load capacity. On the other hand, it is feasible that, when a weak adherence of the geogrid and asphaltic layers happens, displacement and vertical stress become higher; that is, geogrid misplacing or its un-bonding on upper layers through time, subsurface resistant against rutting, will be significantly decreased.

3.4 About Geogrid

Figure 30 shows on the left side a model with full roughness, while the right one shows a μ=0.9 coefficient model.

Figure 30. Outline diagram comparison [Pa] about stress on geogrid between: absolute roughness (left), and one with μ = 0.9 coefficient (right)

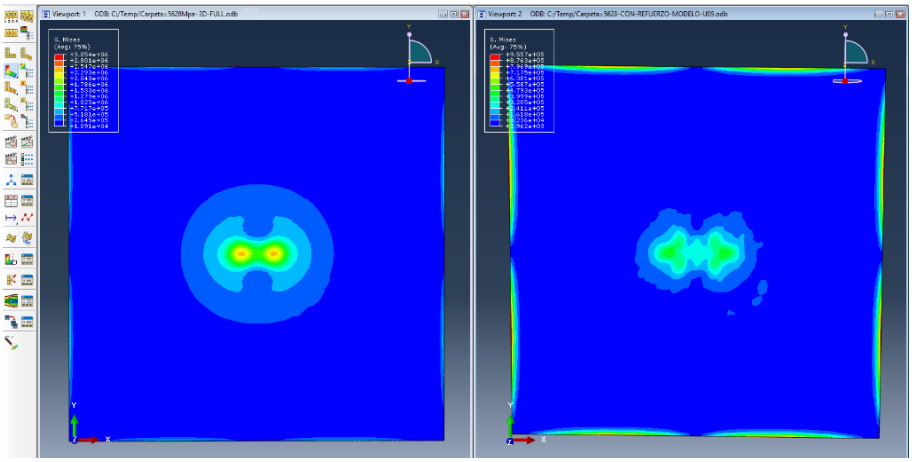

Source: own elaboration.

The figures above show the stress generated by tire load when having a full adherence. They are distributed on a symmetric way in a greater area. This allows a reduction on the max value effort preventing it from focusing on a small area (like on μ=0.9 roughness coefficient). This can generate for the geogrid to overpass its max tension resistance, adding that there is no optimal stress transmission from the previous layer. Considering that, a higher stress value is evident with low roughness coefficient while with adequate adherence such values will be decrease, as proven on figure 31, where effort values are lower when roughness is μ=0.7 (left) or when μ=0.5 (right).

Figure 31. Outlined stress diagram comparison [Pa] on geogrid. Model with a μ = 0.7 coefficient (left) and with a μ = 0.5 coefficient (right)

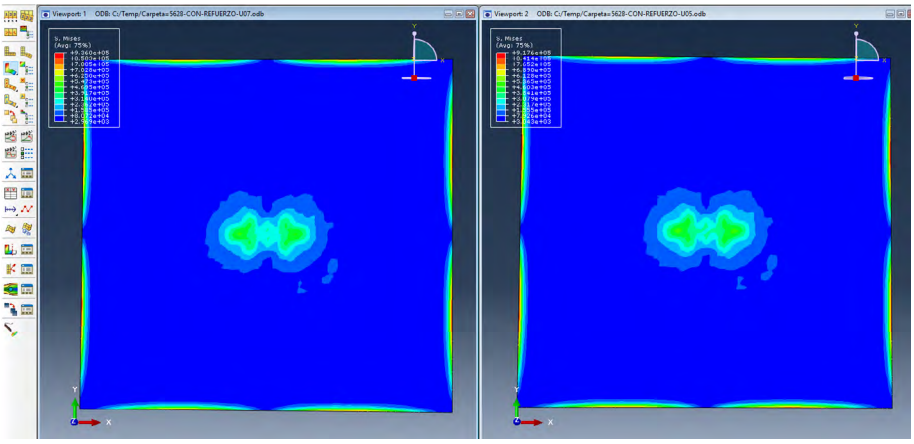

Source: own elaboration.

4. CONCLUSIONS

There is an evident improvement in performance that pavement models have when an appropriate adherence happens between geogrid and asphaltic layers, which means that the structure would last longer and have a better performance.

When there is roughness between the geogrid and the asphaltic layers, both (layers 1 and 2) will work in a monolithic way, giving room to a better inertia element working similarly to a high cant beam. However, when there is loss over the interface adherence, each layer would work separately as having two beams with lower cant. Even the main effect to set a grid is against fatigue failure, this also contributes to slightly reducing failure by rutting when it is fully attached. However, if adherence is lost, the structure is highly prone to deformations on the subsurface.

Graphing vertical stress variances over depth could prove how geogrids (with a high elasticity module of 70,0000 (MPa) holds into the greater effects produced by vehicle loads.

REFERENCES

[1] R. J. Bathurst, "Functions of geosynthetics", IGS, 2015.

[2] A. S. Bustamante, "Evaluación en el Nivel de Resistencia de una Subrasante, con el Uso Combinado de una Geomalla y un Geotextil". Master's thesis. Universidad de Cuenca, 2016.

[3] J. R. Obando, "Desempenho de misturas asfálticas reforçadas com geossintéticos". Ph.D. dissertation. University of Brasilia, Brasilia, BRA, 2016.

[4] J. G. Zornberg, "Sistemas de pavimentos reforzados con geosinteticos", Ingenieria civil, vol. 171, pp. 5-25, 2013.

[5] S. W. Perkins, «Desarrollo de metodos de diseño con geosinteticos para reforzar pavimentos flexibles,» Bozeman, 2004.

[6] M. J. Williamson, "Finite element analysis of hot-mix asphalt layer interface bonding". PhD thesis. Kansas State University, 2015.

[7] J. V. Jimenez, M. M. Theurer, J. C. Rizo and C. Maza, «La geomalla como elemento de refuerzo en pavimentos flexibles,» Ingeniería, Vol. 1, pp. , pp. 63-71, 31 May, 2017.

[8] H. L. Delbono, "Estudio de grillas poliméricas en sistemas anti-reflejo de fisuras bajo solicitaciones dinamicas". PhD thesis. Universidad Tecnológica Nacional, 2014.

[9] N. Sudarsanan, R. Karpurapu and V. Amrithaligam, «Investigación sobre la resistencia de la union de la interfaz de hormigon asfaltico reforzado con geosintetico usando ensayo de corte Leutner,» Construction and buildings materials, vol. 186, pp. 423-437, 2018.

[10] L. G. Loria and P. L. Padilla, "Como reforzar pavimentos flexibles con materiales geosinteticos", Civilizate, no. 5, pp. 39-41, 2014.

[11] PAVCO, Manual de diseño con geosintéticos, Bogota D.C.: Mexichem, 2012.

[12] T. Komatsu, H. Kikuta and Y. Tuji, «Durability assement of geogrid-reinforced asphalt concrete,» Geotextiles and geomembranes, vol. 16, pp. 257-271, 1998.

[13] L. HL and L. H, «Finite elements studies of asphalt concrete pavement reinforced with geogrid,» Enginnering Mechanics, vol. 129, nº 7, pp. 801-811, 2003.

[14] A. A. Bohagr, Finite Element Modeling of Geosynthetic Reinforced Pavement Subgrades. M.S. Thesis. Washington state university, 2013.

[15] Instituto Nacional de Vias, Manual de diseño de pavimentos asfalticos en vias con medios y altos volumenes de transito, Santa Fe de Bogotá, 1998.

[16] H. A. Quintana Rondón and F. A. Lizcano Reyes, Pavimentos. Materiales, construccion y diseño, Bogotá: ECOE ediciones, 2011.

[17] J. C. Á. Tamayo, "Diseño geometrico de la via palmera hasta la estancia y estabilizacion de taludes en la parroquia río negro del cantón baños de agua santa, provincia de Tungurahua". Undergraduate thesis. Universidad técnica de Ambato, 2006.

[18] C. A. B. Bastidas, Conferencias de clase de maestria en ingeniería de pavimentos, Popayan, 2015.

[19] E. Cuelho and S. Perkins, «Estabilizacion de subrasante con geosintéticos,» Transportation geotechnics, vol. 10, pp. 22-34, October, 2016.

[20] L. A. Ricci, "Evaluación de la adherencia entre capas asfalticas con intercapa de geosintético", M.S. thesis, University of Buenos Aires, Argentina, 2011.

[21] J. Giroud y J. HAn, «Desing method for geogrid-reinforced umpaved roads, development of desing method,» Geotechnical and Geoenvirenmental Engineering, vol. 132, July, 2004.